18
Pediatric Malignancies: Synopsis of Current Imaging Techniques

Sabah Servaes[1], Monica Epelman[2], Avrum Pollock[3], and Karuna Shekdar[4]

Key Points

- PET/CT has proven utility in lymphoma, but studies are ongoing regarding its utility with pediatric neoplasms. CT is generally used initially with PET/CT for follow-up.
- Whole-body MRI is a promising technique to evaluate pathology such as metastases without using ionizing radiation with limits regarding specificity and small lesions.
- New MRI techniques are being developed and older techniques are being applied in new ways to improve the evaluation of pediatric neoplasms. MRI can also provide biochemical assessment of lesions.
- Chest CT is required for the staging of sarcomas. Metastases can be evaluated with bone scan and whole-body MRI, and PET/CT is currently under evaluation.

1 Introduction

The imaging evaluation of malignancies is directed towards the assessment of size, location and characterization of the neoplasm. Imaging children necessitates additional attention to the dose of radiation, given the radiosensitivity and the expected longevity of children. This chapter will present some of the latest technologies used to image pediatric malignancies, as well as methods to evaluate the most common pediatric neoplasms.

[1]Department of Radiology, The Children's Hospital of Philadelphia, 34th Street and Civic Center Blvd., Philadelphia, PA 19104, servaes@email.chop.edu

[2]Department of Radiology, The Children's Hospital of Philadelphia, 34th Street and Civic Center Blvd., Philadelphia, PA 19104, epelman@email.chop.edu

[3]Director of Residency and Fellowship Programs, Department of Radiology, Division of Neuroradiology, The Children's Hospital of Philadelphia, 34th Street and Civic Center Blvd., Philadelphia, PA 19104-4399, pollocka@email.chop.edu

[4]Clinical Assistant – Neuroradiology, Hosp. of Univ. of Pennsylvania,, 219 Dulles Bldg., 3400 Spruce St., Philadelphia, PA 19104-4283, karuna.shekdar@uphs.upenn.edu

M.A. Blake and M.K. Kalra (eds.), *Imaging in Oncology.*

2 Overview of Latest Imaging Technologies

2.1 PET/CT

Staging of tumors, as well as response to therapy, is typically assessed by the size of the tumor and nodal location utilizing radiography, ultrasound, MRI and especially CT. With PET functional evaluation increases the diagnostic capabilities. Initially, PET and CT were always performed separately with interpreter comparison or software which retrospectively fused the images. Since 1998 PET/CT machines have minimized the problems which may arise from separately acquired images, such as misregistration due to differences in patient positioning [1]. PET enables clinicians to evaluate the presence of metabolically active tissue and determine the amount of metabolic activity by measuring the ratio of tumor activity concentration to the rest of the body (standardized uptake value or SUV). These measurements help to distinguish benign from malignant tumors, to evaluate the stage of a neoplasm, to evaluate response to therapy, to determine the optimal site for biopsy and to distinguish scar from residual neoplastic tissue following therapy.

Fluorine-18 Fluorodeoxyglucose (^{18}FDG)-PET is the radiopharmaceutical most commonly used clinically. ^{18}FDG is a glucose analogue which localizes to sites where there is active metabolism and increased glucose uptake, such as malignant neoplasms. Glucose and fluordeoxyglucose are transported into cells and subsequently phosphorylated. Metabolism of fluordeoxyglucose is very slow at this point and, therefore, accumulates within the cell at a rate proportional to the rate of glucose metabolism. The one area of exception is in the liver, where fluorodeoxyglucose is readily dephosphorylated.

Blood flow is another important physiologic feature which can be evaluated by measuring the accumulation of a freely diffusible tracer (such as oxygen-15-water), or by detecting markers of angiogenesis with isotop- labeled monoclonal antibodies. Other radiopharmaceuticals are currently being investigated for clinical utility [2].

In addition to increased uptake in malignant neoplasms, increased uptake may occur in normal tissues and benign entities that must be recognized. The gray matter of brain parenchyma has high ^{18}FDG uptake because of its high glucose metabolism and, therefore, there is limited clinical benefit for intra-axial malignant disease, although facial and neck abnormalities may be detected. Liver, spleen and bone marrow also show homogeneous low-grade uptake, but malignant processes can still be seen within these tissues. Myocardial uptake is variable and fasting prior to an exam is helpful because the heart then uses fatty acids for metabolism. However, distinguishing myocardial activity from lymph nodes may be challenging. Normal lymphoid tissue in Waldeyer's ring and pediatric thymic tissue have moderate uptake. Following chemotherapy in children and young adults, thymic rebound also demonstrates increased ^{18}FDG uptake. Within the gastrointestinal tract activity is typically low in the esophagus, but benign entities such as esophagitis can increase ^{18}FDG uptake. Similarly, gastritis can cause increased ^{18}FDG uptake in the stomach. Although there is minimal uptake in the small bowel, the colon and particularly the cecum demonstrate avid uptake of ^{18}FDG. ^{18}FDG

is excreted renally and, therefore, malignancies involving the urinary tract have limited clinical benefit. Bladder catheterization and appropriate placement of the bag which collects the urine are important in the evaluation of the pelvis. Children may also demonstrate increased ^{18}FDG uptake in brown fat. To decrease skeletal muscle uptake patient motion, including speech, must be minimized and the temperature of the room adjusted to prevent shivering.

Pathologic causes of increased ^{18}FDG uptake include benign entities such as inflammation or infection. Bone which is healing from trauma or arthritis causes increased ^{18}FDG uptake. Lymph nodes may demonstrate increased ^{18}FDG uptake in tuberculosis and sarcoidosis. Similarly, recent infection, surgery or extravasation of radiotracer may cause the lymph nodes draining the involved region to demonstrate increased ^{18}FDG uptake.

Because the duration of time required for acquiring the PET images is more than 20 minutes and the CT can be obtained within a single breath-hold, the region about the diaphragm and nodules within the lungs are difficult to assess secondary to misregistration. Other technical factors which impact interpretation are the use of oral and intravenous contrast agents. High density oral contrast causes artifact, similar to metallic implants. Analogously, the arterial phase of intravenous enhancement causes more difficulty than venous phase. There is ongoing debate regarding the best technique, ranging from the absence of any contrast to those advocating for both oral and intravenous contrast [3-8].

Among the pediatric malignancies most often imaged with PET/CT are: Neuroblastoma [9], lymphoma [10-12] and soft tissue sarcomas [13, 14]. One advantage of PET/CT over CT alone is that PET provides information regarding the functionality of lymph nodes, allowing for appreciation of normal sized nodes that are involved in disease and the realization that some large lymph nodes are merely reactive. (Fig. 18.1) One of the pitfalls in the evaluation with PET is increased ^{18}FDG uptake in nonneoplastic disorders [15]. Although there are issues regarding some of PET/CT's findings and difficulties with interpretation, the initial studies indicate that PET/CT will play an important role in pediatric malignancy evaluation [16, 17].

3 Whole-Body MRI

Turbo short tau inversion recovery (STIR) whole-body MR imaging is a promising technique to study the entire body in a reasonable amount of time, and without utilizing ionizing radiation, a feature which is especially important in this population, in whom serial longitudinal follow-up studies are needed. This procedure has been used in pediatric oncology mainly for the detection of metastases or total tumor burden assessment [18-27]. Whole-body MRI has been shown to have better diagnostic accuracy in lesions that do not induce osteoblastic response, and is particularly helpful in the detection of bone marrow lesions, as compared with conventional skeletal scintigraphy and plain radiographs [18, 19, 25, 28]. However, whole-body MRI has other potential roles. Whole-body MRI may be particularly helpful in the

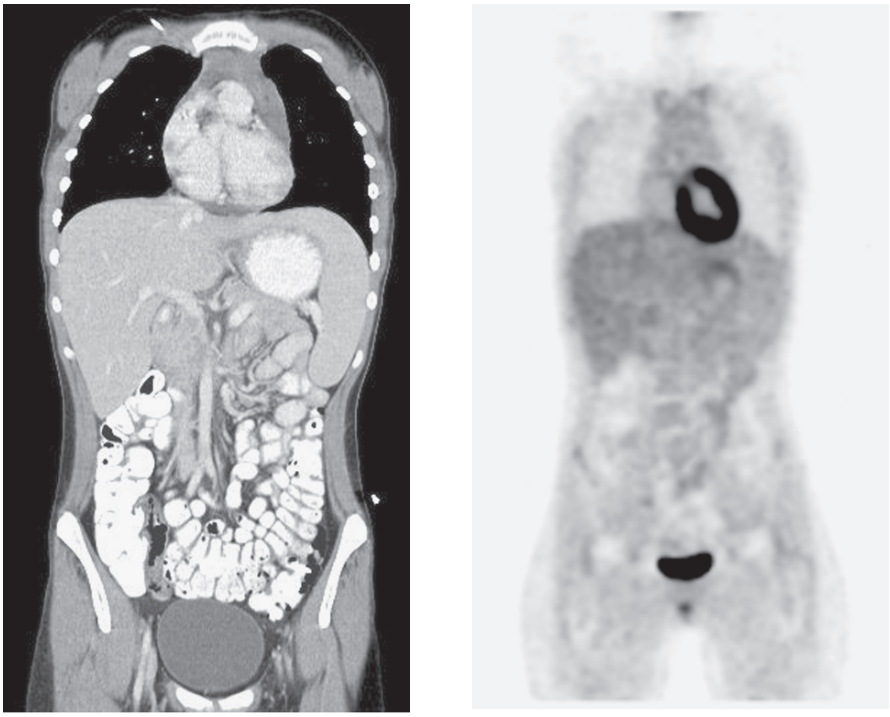

(a) **(b)**

Fig. 18.1 (**a**) Coronal CT reformat of the chest, abdomen and pelvis in this girl with Hodgkin's lymphoma and a mediastinal mass which is decreasing in size. (**b**) PET confirms that there is no uptake in the residual mediastinal mass

evaluation of multifocal avascular necrosis, especially following treatment with high-dose steroids. The detection of post-transplantation lymphoproliferative disorders, mainly after bone marrow transplantation, is another indication for whole-body MRI [29]. If follow-up whole-body MRI shows no response or tumor progression, prompt modifications in therapy become feasible due to this ability to evaluate initial treatment response [19].

Whole-body MRI can be performed on almost every body MRI system and may potentially replace other imaging studies, especially given recent improvements to decrease acquisition time. Once localizing scans are acquired, the entire body is imaged from the vertex to the heels by coronal turbo STIR sequences obtained in multiple overlapping stations. The field of view is adjusted to the size of the patient. The slice thickness is chosen to allow for complete anterior-to-posterior coverage [22, 25]. By using the turbo STIR sequences each set of coronal images may be acquired in less than four minutes, which can be further reduced to less than a minute if breath-hold techniques are applied [25]. Many parameters have not been standardized including, among others, the type of coil used (body versus surface

coils), imaging techniques to reduce motion artifacts (e.g., respiratory triggering) and imaging plane selection [19].

The turbo STIR sequence is sensitive to soft tissue and skeletal pathology, due to the resultant added proton density (PD), T1 and T2 contrast with inherent suppression of signal from fat. Most pathologic tissues are proton-rich and have prolonged T1 relaxation and T2 decay times, resulting in high signal on turbo STIR images. This signal hyperintensity within proton-rich tumor metastasis becomes particularly noticeable against a background of hypointense suppressed fatty marrow, affording ease of image interpretation [22, 25, 26].

The turbo STIR sequence is sensitive to soft tissue and skeletal pathology, due to its added proton density, T1 and T2 contrast with inherent suppression of signal from fat without needing intravenous contrast administration. Most pathologic tissues are proton-rich and have prolonged T1 relaxation and T2 decay times, resulting in high signal on turbo STIR images. This signal hyperintensity within proton-rich metastastes becomes particularly noticeable against a background of hypointense suppressed fatty marrow, or isointense to muscle normal hematopoietic marrow, allowing ease of image interpretation [22, 25].

However, there are some limitations to whole-body MRI. STIR techniques are highly sensitive for detecting of pathologic lesions, but not specific for malignancy. Inflammatory, infectious, traumatic and necrotic changes, as well as benign lesions such as cysts and hemangiomas, cannot be differentiated from neoplastic lesions and appear hyperintense on STIR imaging. Whole-body STIR MR imaging may also be limited in the evaluation of oncologic patients following treatment, in that therapy-induced marrow changes such as edema, necrosis, fibrosis or red marrow hyperplasia (related to anemia or treatment with granulocyte-colony stimulating factor), cannot be differentiated from viable tumors. Although parenchymal lesions in the liver, spleen, kidneys, lungs and brain are readily detectable, smaller parenchymal lesions may be missed due to the low spatial resolution of the whole-body technique [19, 22]. PET/CT represents the greatest challenge to whole-body MRI. On the other hand, the major disadvantage of PET/CT is the increased radiation exposure sustained by young patients which may result in high cumulative radiation doses in children in whom oncologic imaging is performed repetitively and over relatively short time intervals. These may result in a higher cancer mortality risk, since children are more radiosensitive than adults [19, 30]. Therefore, whole-body MRI offers an alternative as a non-ionizing imaging modality for staging and monitoring tumor response [20].

4 CT Angiography – MRI Angiography

Although vascular invasion in childhood neoplasm is uncommon, vessel invasion may occur, particularly in Wilms' tumors [31], soft tissue sarcomas and primary bone tumors [32]. Nonetheless, decision-making before surgical treatment in patients with

neoplasms, requires accurate delineation of the presence and level of vascular involvement. Unlike in adults, the role of CTA and MRA in pediatric oncologic imaging is yet to be defined. Many of the questions raised in conventional CT or MRI exams can be solved with Doppler ultrasound (US). However, CTA or MRA are indicated in cases when US results are inconclusive, confirmation is required before surgery to avoid complications or if clinical suspicion exists despite normal US results. The lesion's appearance and its relationship to the vasculature is of use to the surgeons, particularly prior to resection of tumors encasing the renal arteries. Vascular mapping, by means of CTA or MRA, is extremely helpful for careful and safe surgical planning, and has a potential role in the preoperative planning of hepatoblastoma. The not-uncommon replaced right hepatic artery off the superior mesenteric artery is easily identified in the arterial phase, if right hepatectomy is required. While in the portal venous phase, the assessment of portal venous occlusion, cavernous transformation or portal vein tumor thrombus becomes more conspicuous. In addition, vascular mapping of the aortic vasculature, including accessory renal arteries, is of use in cases of Wilms' tumor, especially if nephron sparing surgery is required, or in the surgical planning of subadventitial dissection of neuroblastoma and extensive retroperitoneal lymphadenopathy (Fig. 18.2) [20, 70, 71].

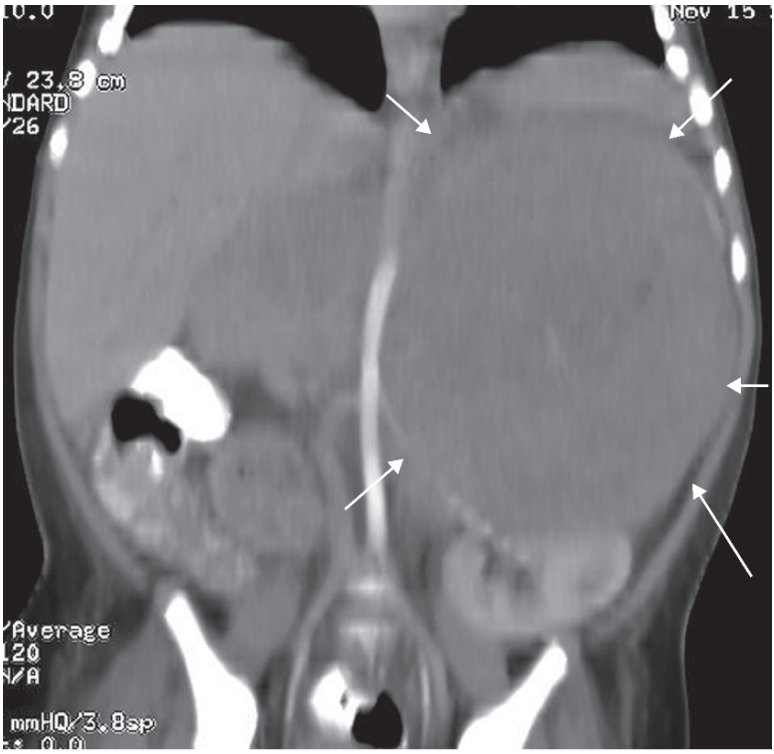

Fig. 18.2 Coronal CT reformat of the abdomen and pelvis in this 10-month-old with neuroblastoma

5 MR Urography

With recent improvements in MRI equipment, including the development of faster gradients, stronger magnetic fields and parallel imaging, MR urography is now being used not only for the delineation of genitourinary anomalies, but also for the precise anatomic delineation of either intrinsic or extrinsic neoplasms affecting the genitourinary tract. In the pediatric population, and following initial US evaluation, MR urography, in combination with standard MR imaging, has the potential to reduce the need for intravenous pyelography, abdomino-pelvic CT and retrograde pyelography as a noninvasive, non-ionizing imaging option (Fig. 18.3) [33, 34].

6 MRI Spectroscopy

Proton MR Spectroscopy (MRS) is a powerful technique used to evaluate CNS neoplasms, which provides metabolite information that helps further characterize a tumor. Specifically, MRS is useful in differentiating tumors from normal tissue, and from other pathologies producing similar abnormal brain signal. It is useful in determining

Fig. 18.3 Coronal image from an MRU in this 5-year-old boy with prostatic rhabdomyosarcoma, which caused bilateral pelvicaliectasis, bilateral ureterectasis and a urinoma on the right

the tumor grade and in guiding the appropriate site for biopsy [35]. Another important use of MRS is in distinguishing radiation necrosis from recurrent neoplasm.

MRS interrogates the chemical structure of areas in the brain. Spectroscopic data is obtained from a small volume of brain (approximately 1 square cm) to prevent the averaging of other normal metabolites within that volume. The sampling area or the cube of tissue which is evaluated is called a voxel. Single-voxel and multi-voxel MR spectroscopy techniques are utilized. Normal brain tissue has a characteristic neurochemical signature, depending on its location and the age of the patient [36]. MR spectroscopy can detect the various neurochemical spectral peaks. Among the neurochemicals which are most important in the analysis of brain tumors are N-acetyl acetate (NAA), choline compounds (Cho), creatine (Cr), lactate (Lac), myo-inositol (Myo) and amino acids (AA) [36]. NAA is considered a marker of normal functioning neurons. NAA is depleted in disorders which destroy the neuronal cells. Choline is an important component of the cell membrane. Choline levels are markers for cell membrane turnover which is increased in brain tumors and also in other disorders such as infection, inflammation and demyelination. Creatine peak results from creatine and phosphocreatine compounds which are high-energy buffers for ATP synthesis. Creatine is seen to be depressed in high-grade tumors which have an overwhelming energy requirement due to the hyper-proliferative tumor cells. In necrotic portions of the tumor, creatine is nearly depleted due to cell death. Lactate is a marker of anaerobic metabolism and, therefore, is elevated in high-grade or necrotic neoplasms, ischemia and in areas of injured brain tissue.

MR spectroscopy is useful for grading astrocytic neoplasms based on the different magnitudes and ratios of the metabolites in the tumor [36]. Typically the NAA is decreased and choline is elevated (Fig. 18.4). The more the metabolite peaks vary

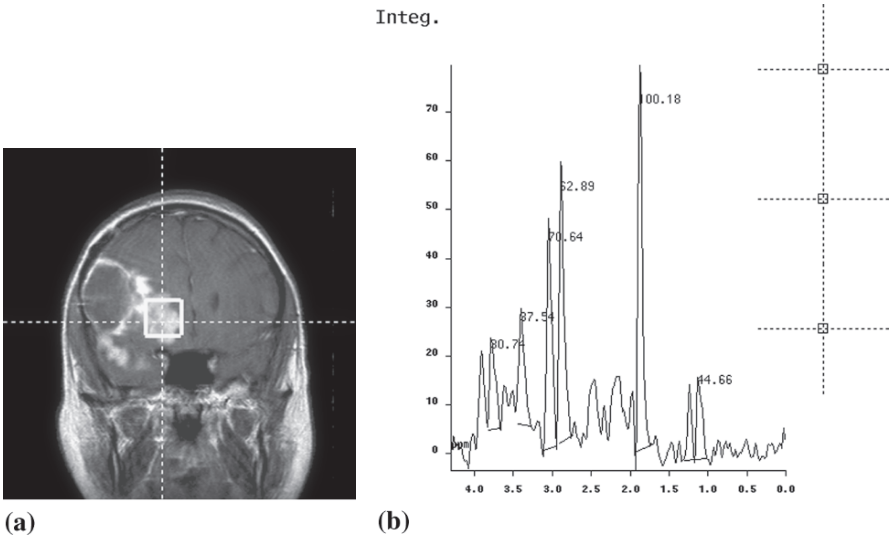

(a) (b)

Fig. 18.4 (**a**) Localizing post-contrast T1 coronal MR image of the brain in a patient with glioblastoma multiforme. (**b**) The control spectrum demonstrates the normal spectral peaks

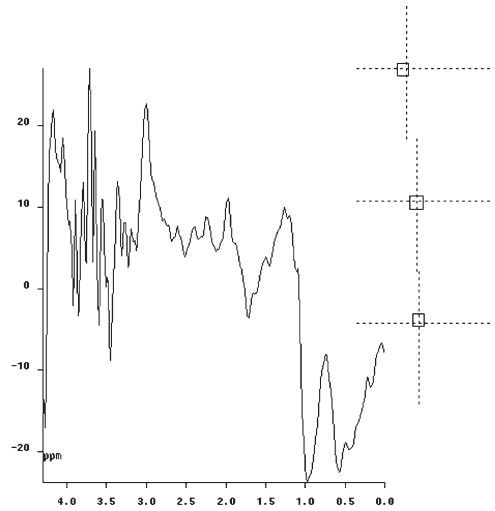

Fig. 18.4 (continued) (**c**) The voxel centered within this patient's tumor demonstrates loss of the normal spectral pattern within the tumor mass

from the normal values, the more aggressive the tumor. Increased lactate is associated with more aggressive neoplasms. Some brain tumors have characteristic spectral patterns, e.g. meningiomas, which have an alanine peak not seen in other tumors. In radiation injury, usually in the early stages, there is increased choline from destruction of the cellular membrane, but a normal NAA peak. Without the presence of active tumor there is usually global decrease in the peaks of NAA, choline and creatine in areas of treatment-related injury. Elevation of choline and reduction of NAA are suggestive of tumor recurrence.

It is important, however, to realize that some tumors (such as juvenile pilocytic astrocytoma, the most benign and relatively common pediatric brain tumor) can demonstrate elevated choline and lactate with reduced NAA, a pattern which is seen with higher grade tumors [37]. Nonneoplastic disorders comprised of inflammatory processes, demyelination plaques, tuberculomas and encephalitis have MR spectroscopy features which are nearly identical to neoplasms. Hence, it is important that MR spectroscopy data be evaluated not in isolation, but in conjunction with anatomic MR imaging. MR spectroscopy findings may remain nonspecific. Further, spectroscopy data can be technically inadequate depending upon the size and the location of the neoplasm. Spectral data can be contaminated by adjacent CSF or fat in the calvarium/skull base. Voxel sampling may be inadequate if the tumor size is small or is extremely peripheral in location.

MR spectroscopy is a valuable tool which supplements conventional MR imaging. MR spectroscopy imaging improves imaging of pediatric brain tumors because it gives a biochemical assessment of the tumor, and may distinguish residual or recurrent tumor from radiation necrosis [38].

7 MRI Perfusion

With the availability of high strength MRI gradients and ultrafast imaging sequences and, specifically, echo planar imaging, MRI perfusion imaging can be utilized for CNS neoplasms with a very small scan time penalty. It is possible to evaluate the dynamic changes which reflect tissue perfusion, relative cerebral blood volume (rCBV), cerebral blood flow (CBF) and mean transit time (MTT). Several methods can be utilized to derive perfusion parameters with MR imaging. Commonly, MRI perfusion imaging is performed using intravenously administered contrast medium (e.g., gadolinium-DTPA). The dynamic signal changes are due to passage of the bolus of contrast through the cerebral vessels into the capillary bed. The degree of signal loss is proportional to the concentration of gadolinium in the tissues of interest. This information is then utilized to generate perfusion maps of the area's hemodynamic parameters [39].

Studies have shown that data obtained from perfusion MRI correlate with the degree of tumor angiogenesis and, hence, may be good predictors of the aggressive nature of the tumor. Therefore, tumors which have larger rCBV correlate to higher-grade aggressive neoplasms [40].

Traditionally, contrast enhancement has been used as a crude marker of tumor vascularity. However, contrast enhancement reflects the breakdown in the blood-brain barrier and is not always representative of tumor vascularity. On the other hand, increased rCBV represents areas of increased vascularity in an aggressive neoplasm. Studies have shown that areas of increased rCBV may not always correspond to the contrast-enhancing portion of the tumor. Perfusion-weighted MR imaging is a more sensitive, noninvasive modality to predict tumor angiogenesis and vascularity [40].

Besides grading neoplasms, perfusion MRI can be used to guide stereotactic biopsies [41]. This capability is especially important in heterogeneous tumors. Prior to perfusion MRI, most of the brain tumor stereotactic biopsies would be directed to areas of contrast enhancement. Using perfusion MRI the areas within the tumor that demonstrate high rCBV can be identified as being the most aggressive, thereby guiding the interventionalist/surgeon to biopsy in this region.

Serial perfusion-weighted MRI studies during therapy can noninvasively assess the changing tumor biology and dynamics. This function can potentially be used to determine optimal chemotherapy dosing [42].

Another important application of perfusion MR imaging is distinguishing treatment-induced brain injury from residual or recurrent neoplasm [41]. This difference in the pathophysiology of injured brain versus tumor tissue is exploited by perfusion MR imaging. With brain injury that results from damage to the endothelium, the end result is hypo-perfusion of the affected tissue, whereas growing tumor cells have an increased amount of blood supply for their proliferation and are associated with an increased rCBV. Studies have shown that these results, based on perfusion MRI, correlate well with identification of treatment-related brain injury and residual or recurrent tumors [41, 43]. MRI perfusion imaging is limited, especially in the younger pediatric population, by the need for adequate sized intravenous access to achieve an adequate contrast bolus.

In summary, perfusion MR imaging is a valuable diagnostic tool to enhance anatomic MR imaging. It is clinically useful in accurately grading tumors, guiding stereotactic biopsies and helping distinguish between residual/progressive neoplasms from treatment-related brain injury. The potential use of MRI perfusion for mapping chemotherapeutic agent distribution and dosages are currently being assessed.

8 Diffusion MR Imaging

Diffusion-weighted MR imaging has been utilized for many years in neuroradiology, and recently has been promoted for abdominal imaging [44-46]. The studies suggest that alteration in water motion between compartments or diffusion, which is impacted by tumor response to treatment, can be detected with this MRI sequence and, thereby, monitor neoplastic processes. This technique, which measures the motion of water protons, can be effectively performed even with patient motion associated with breathing freely [44]. This technique has been used to distinguish a neoplastic process from a lymphatic malformation in a child [45]. Although more studies are needed, these results suggest that diffusion-weighted MR imaging will provide an alternative method to monitor response to therapy in oncology patients without using ionizing radiation.

9 Applications of Modern Imaging Techniques in Pediatric Malignancies

9.1 Leukemia and Lymphoma

Leukemia is the most common childhood malignancy and lymphoma is the third most common. Together, these malignancies constitute nearly half of all childhood cancer. Approximately one-third of all childhood malignancy is due to leukemia, primarily acute leukemia. Acute lymphoblastic leukemia (ALL) peaks at two to three years of age, and acute myeloid leukemia (AML) peaks during the first two years of life and again during adolescence. Radiation exposure is one of the important risk factors associated with the development of leukemia [47, 48]. Lymphoma constitutes 10 percent to 12 percent of all childhood cancer. Lymphoma is classified into Non-Hodgkin's Lymphoma and Hodgkin's Lymphoma [49]. Hodgkin's Lymphoma is the most common lymphoma, and, because of the high frequency in adolescence, has a greater incidence than brain neoplasms, which represent the second most common childhood malignancy.

There are many imaging features which overlap between leukemia and lymphoma and, therefore, both are often suggested together in differentials provided with radiological interpretation. Lymphoma is the most common etiology for a mediastinal mass, which may be easily seen on chest radiographs (Fig. 18.5), and

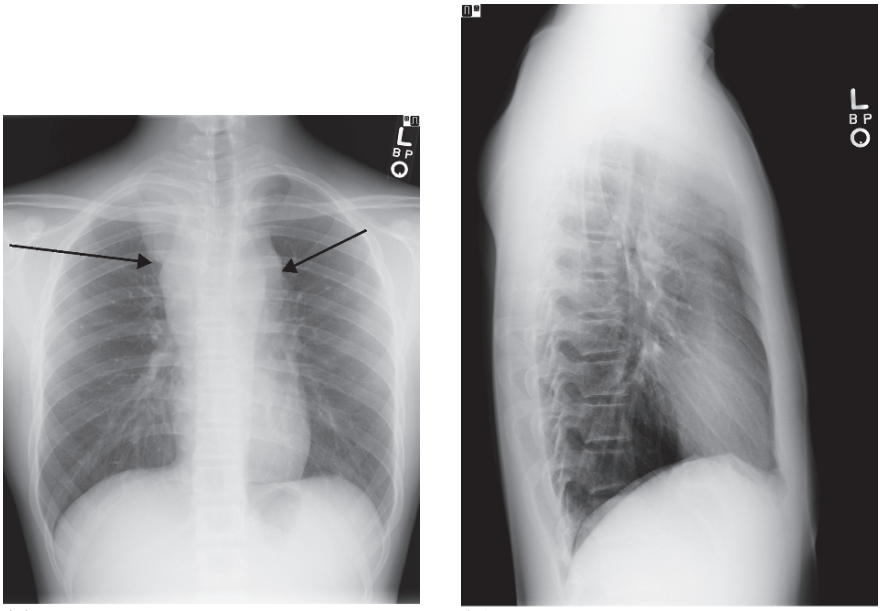

(a) (b)

Fig. 18.5 (**a**) PA and (**b**) lateral chest X-ray demonstrating a mediastinal mass in this patient with Hodgkin's lymphoma

leukemia may also result in a mediastinal mass. CT is often used in the evaluation of a mediastinal mass. However, PET/CT plays an increasingly important role in imaging these patients [10-12, 50-56]. Gallium scans may provide similar information, but not with the same anatomic localization as PET/CT, and some studies indicate that gallium scanning is inferior to PET/CT [57-60].

Whole-body MRI has also been shown to be of value [61], providing evaluation without the use of ionizing radiation, which is particularly important in the pediatric population [62]. Although MRI offers the advantage of providing different signal with differing tissue characteristics, determination of lymph node pathology remains based upon size criteria, as with CT.

Osseous abnormalities are also found with leukemia and lymphoma. On radiographs, metaphyseal lucencies are referred to as leukemic lines. (Fig. 18.6) MRI is especially sensitive at detecting marrow infiltration of leukemia and lymphoma. Fluid-sensitive sequences such as T2-weighted or STIR demonstrate abnormally increased signal, whereas T1-weighted images demonstrate decreased signal secondary to the increased water content of tumors [61]. (Fig. 18.7)

The pediatric survival rate for lymphoma is 75 percent in the United States [63]. This cure rate is dependent upon accurate staging, for which there is a promising future of continued improvement.

Fig. 18.6 AP X-ray of the ankle in this child with ALL demonstrates metaphyseal lucency

10 Central Nervous System

The prevalence rate for all primary brain and central nervous system tumors was estimated to be 9.5 per 100,000 in the United States for the year 2000 [64]. As with any cancer, early detection is essential to achieving a positive outcome. Cross-sectional imaging, e.g., CT and MRI, is the mainstay in diagnosing central nervous system tumors. CT is most often the initial imaging study obtained in the evaluation of suspected brain tumors. CT scanning involves ionizing radiation and should be used judiciously in the pediatric population. CT is especially valuable when a rapid study is needed to assess for hemorrhage, ventricular size or mass effect. With its multiplanar capability and excellent high spatial resolution, MRI is a superior imaging modality in the diagnosis and characterization of brain tumors, as well as in the follow-up to assess response to treatment. (Fig. 18.8) The development of new pulse sequences and ultrafast sequences has allowed for high resolution images to be obtained in a short time, which is particularly critical in pediatric imaging because it may obviate the need for sedation. MRI is the modality of choice in imaging spinal cord tumors. CT scan is a useful tool for assessment of bony vertebral body tumors. However, evaluation of spinal canal extension and cord involvement is best assessed with MRI.

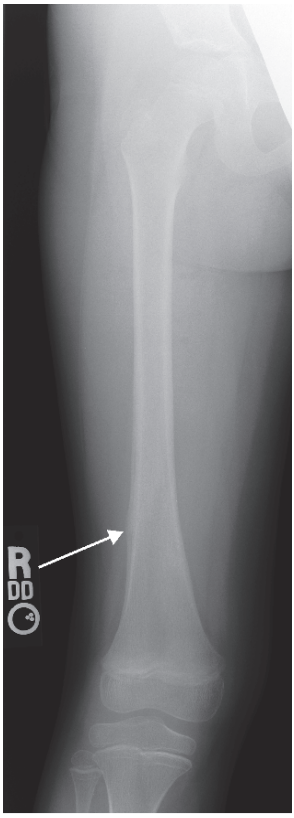

(a)

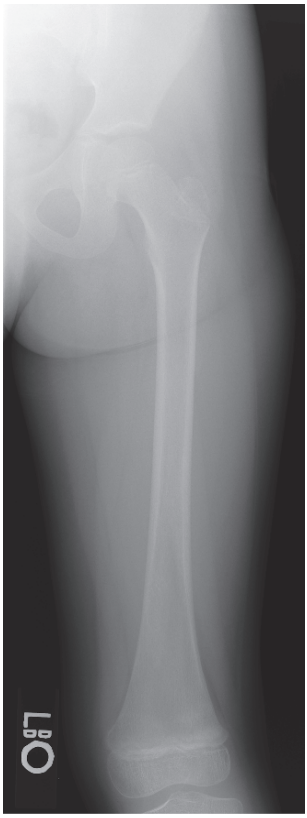

(b)

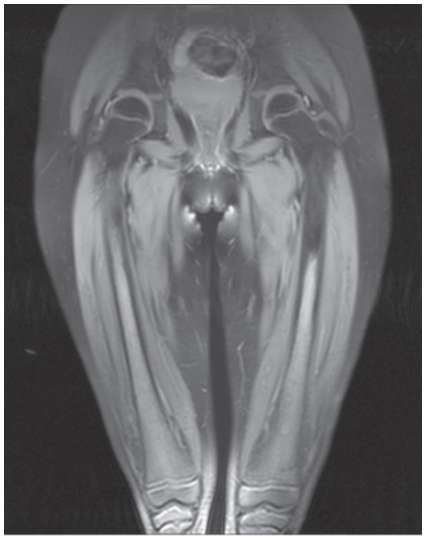

(c)

Fig. 18.7 AP X-ray of the bilateral femurs, demonstrating periosteal reaction on the right (**a**) secondary to a healing fracture and a normal left (**b**) in this patient with lymphoma. (**c**) The marrow infiltration is only appreciated with the MRI (coronal proton density)

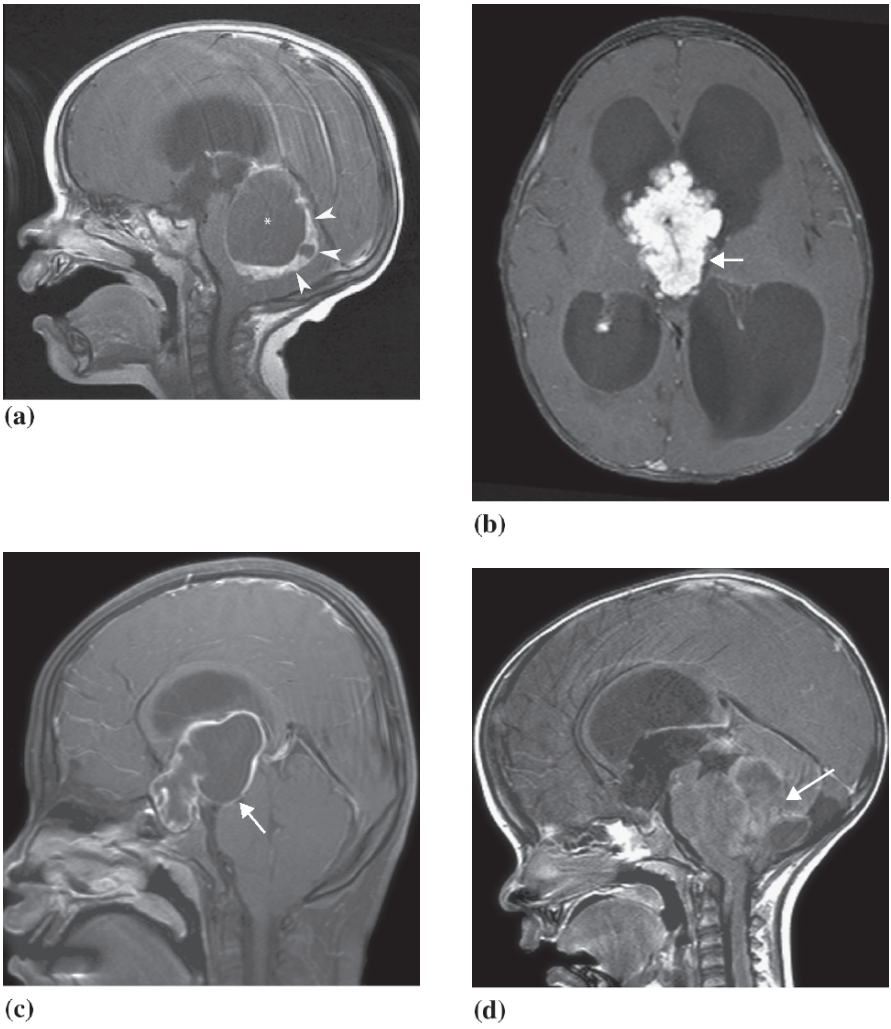

Fig. 18.8 (**a**) T1 post-contrast midline sagittal view of the brain of a child with cerebellar astrocyoma. Note the large cyst (asterisk) centered within in the cerebellum surrounded by a rind of rim enhancing tumor (arrowheads). (**b**) T1 post-contrast fat-saturated axial view of the brain of a child with choroid plexus papilloma. Note the intensely enhancing frond-like tumor centered with the region of the third ventricle, with resultant hydrocephalus. (**c**) T1 post-contrast fat-saturated sagittal view of the brain of a child with craniopharyngioma. Note the suprasellar cystic lesion with rim enhancement, extending cephalad into the region of the third ventricle. (**d**) T1 post-contrast midline sagittal view of the brain of a child with medulloblastoma of the posterior fossa

MR imaging is extensively used in the diagnosis and follow-up of pediatric patients with brain tumors. However, conventional MR imaging does not provide information about the tissue biochemistry or grading of malignancy. An additional shortcoming of MR imaging is incomplete estimation of the extent of the tumor

[65]. Frequently a stereotactic biopsy, an invasive procedure, must be performed to obtain this information. The advanced imaging techniques of MR spectroscopy and MRI perfusion with ADC mapping can provide valuable information about tumor extent, tumor biochemistry and hemodynamics. These are noninvasive imaging tools which supplement the important anatomic information obtained by conventional gadolinium-enhanced MR imaging.

11 Neuroblastoma

The proper diagnostic imaging work-up for neuroblastoma is in constant evolution. Neuroblastoma has a primary location in the adrenal glands or sympathetic chain. Distant metastatic lesions at the time of presentation are seen in approximately 70 percent of children with abdominal neuroblastoma, with the most commonly affected sites being the bone marrow, followed by the lymph nodes, the liver and skin [66].

Conventional radiographs and ultrasound are routinely obtained in children with a suspicious space-occupying lesion. Chest radiographs may reveal a posterior mediastinal mass. Calcification may be seen in at least 30 percent of cases [67]. Ultrasound may show the solid nature of the tumor, which is usually of mixed echogenicity. Contrast-enhanced CT provides further detail on tumor architecture, extent of local disease and distant metastasis. The typical appearance is that of a large suprarenal mass with calcifications. MRI is particularly helpful in determining extension into the spinal canal. Metaiodobenzylguanidine (MIBG) scan is highly specific and sensitive for evaluating bone and bone marrow disease as MIBG is taken up by most neuroblastomas, but not by normal bone [68]. Additional use of technetium 99 m methylene diphosphonate bone scan is advocated by many since it may virtually eliminate any false negative MIBG results [69].

Eventually, confirmation or exclusion of the diagnosis of neuroblastoma is made with examination of tissue obtained by bone marrow aspiration or biopsy of primary or secondary disease.

Metastatic lesions in the skin and lymph nodes are typically amenable to open biopsy. In primary tumors fine needle aspiration may provide reliable diagnosis; however, small sample size generally precludes important immunohistochemical and cytogenetic analysis. FDG-PET and whole-body MRI appear to be promising techniques [20]. Whole-body MRI is currently under investigation *(www.acrin.org)*.

12 Wilms' Tumor

Ultrasonography (US) is frequently the first imaging modality obtained. Whenever Wilms' tumor is suspected, the inferior vena cava (IVC) should be carefully scrutinized for tumor thrombosis, since unrecognized caval thrombosis may result in fatal

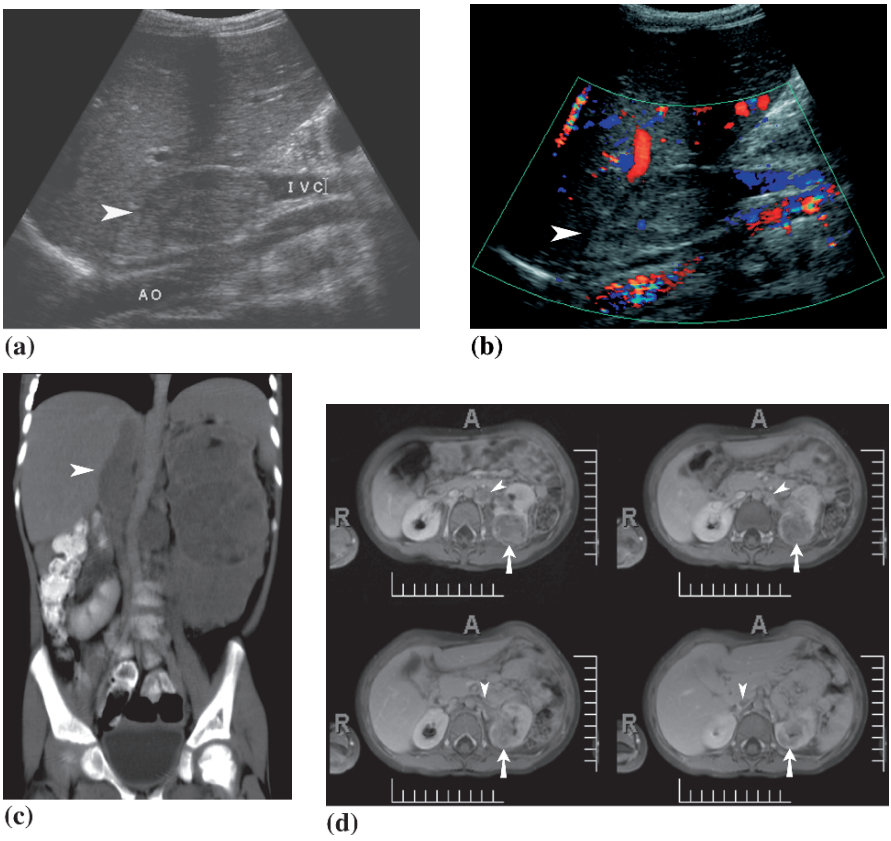

Fig. 18.9 (**a**) Gray scale ultrasound of a 4 year-old girl with left Wilms' tumor demonstrates tumor invasion (arrowhead) of the IVC. AO = Aorta. (**b**) Color Doppler demonstratestumor (arrowhead) within the IVC. (**c**) Coronal CT reformat depicts tumor within the IVC (arrowhead). (**d**) Axial post-contrast MRI demonstrates tumor in the renal vein and IVC (arrowhead) and in the left kidney (arrow)

pulmonary embolus while cross-clamping the IVC during nephrectomy (Fig. 18.9) [20, 70, 71].

CT scan is currently the standard modality for diagnosis. CT is comprehensive, readily available and fast and, therefore, can possibly be performed without sedation. With multidetector scanners reconstructions/reformations in coronal and sagittal planes can assist in surgical planning of nephron-sparing surgery. CT depicts features of the renal lesion, determines the anatomic extent of the tumor and assesses the presence of a normal contralateral kidney versus bilateral tumor involvement. The scan should be obtained during the portal phase of enhancement at 70 seconds following the administration of intravenous contrast. At this point the renal cortex and medulla are attenuating; however, Wilms' tumors are usually hypo-attenuating to normal kidney parenchyma during this phase of

enhancement, allowing for effortless identification of even subcentimeter lesions (Fig. 18.9C) [72].

The role of chest CT for the work-up and later management of pulmonary metastases remains controversial [72-74]. Traditionally, chest involvement is considered positive, if pulmonary nodules are identified on chest radiographs. It is expected that the Children's Oncology Group (COG) will list chest CT as the modality of choice for the evaluation of pulmonary metastasis.

MRI is suggested for the follow-up of bilateral lesions and nephroblastomatosis, as MRI can identify nephrogenic rests as small as 4 mm [20, 75, 76]. This ability is of significant value because it may obviate the need to perform contralateral exploration. Hence, MRI has the potential to replace CT as the pre-surgical imaging modality of choice in the evaluation of Wilms' tumor (Fig. 18.9D) [20, 72].

13 Sarcoma

Rhabdomyosarcoma, osteosarcoma and Ewing's sarcoma are the most common sarcomas in children [9]. Rhabdomyosarcoma is the most common soft tissue sarcoma, with 350 new cases per year in the United States [77]. Osteosarcoma is the most common primary malignant bone tumor and Ewing's sarcoma is the second [78]. Rhabdomyosarcomas are subcategorized into two groups: embryonal rhabdomyosarcoma typically found in children less than six years of age and which constitutes 80 percent, and the remaining 20 percent are alveolar rhabdomyosarcoma typically found in children over six years of age [9]. The incidence of osteosarcoma is 5.6 per million children in the United States [9]. Most osteosarcomas arise from the medullary cavity of the metaphyses of long bones, predominantly about the knee. Although Ewing's sarcoma is the second most common primary malignant bone tumor, the incidence is 225 each year in people under 20 years of age in North America [78]. Ewing's sarcoma occurs most frequently in flat bones or the diaphysis of long bones.

Staging of rhabdomyosarcoma requires assessment of the primary tumor size, location and invasiveness, and is typically done with CT or MRI [77]. The evaluation for metastatic disease includes chest CT and another modality for marrow infiltration such as bone scan or whole-body MRI; PET/CT is not yet part of routine staging for rhabdomyosarcoma, but is currently being investigated [61, 77].

The initial and the critical diagnostic imaging study in the evaluation of an osseous abnormality is a plain radiograph obtained in two orthogonal planes. Radiographs are crucial in making the diagnosis of an osseous lesion. MRI is the other modality of choice (Fig. 18.10). One of the goals of MRI is to evaluate the regional nerves and vessels. Imaging the entire bone is of the utmost importance in osteosarcoma to determine if skip lesions are present. One limitation with MRI is the inability to distinguish between edema surrounding the tumor and the actual extent of tumor. MRI frequently reveals adjacent soft tissue mass as part of Ewing's sarcoma. Chest CT is typically performed to evaluate for metastases in both

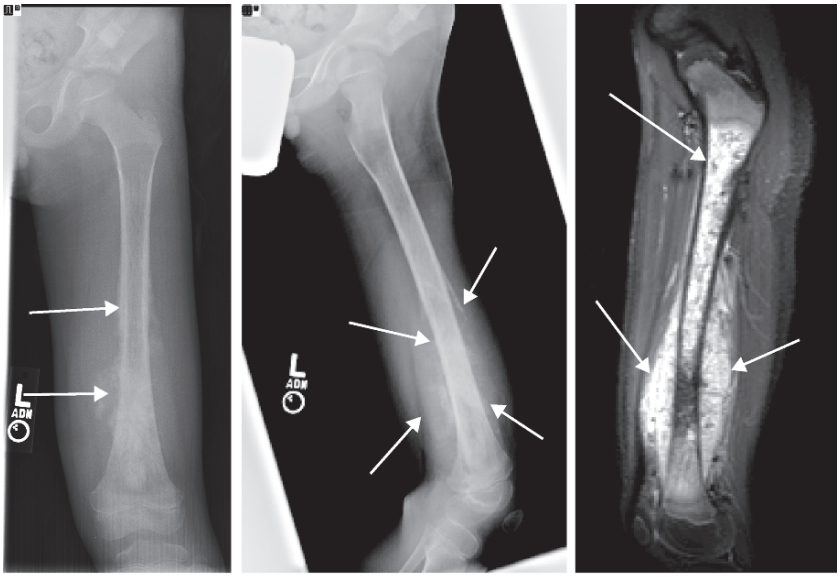

Fig. 18.10 AP (A) and lateral (B) X-rays of the left femur demonstrate periosteal reaction and the aggressive appearance of this osteosarcoma. (C) MRI was performed to evaluate the extent of the lesion and for skip lesions (sagittal STIR)

osteosarcoma and Ewing's sarcoma. Whole-body ^{99m}Technetium bone scan, PET/CT and whole-body MRI have been utilized to determine the presence of osseous metastases. A 2001 study comparing these techniques demonstrated PET/CT to be the most sensitive modality, followed by whole-body MRI [79].

Conclusion

CT and MRI imaging provide crucial information in childhood cancers. Currently, research is ongoing to further define the role of PET/CT imaging in childhood malignancy although its role in imaging subjects with lymphoma has been established.

References

1. Berry JD, Cook GJ. Positron emission tomography in oncology. Br Med Bull 2006.
2. Juweid ME, Cheson BD. Positron-emission tomography and assessment of cancer therapy. N Engl J Med 2006;354:496-507.
3. Dizendorf EV, Treyer V, Von Schulthess GK, Hany TF. Application of oral contrast media in coregistered positron emission tomography-CT. AJR Am J Roentgenol 2002;179:477-81.

4. Rodriguez-Vigil B, Gomez-Leon N, Pinilla I, et al. PET/CT in lymphoma: prospective study of enhanced full-dose PET/CT versus unenhanced low-dose PET/CT. J Nucl Med 2006;47:1643-8.
5. Schaefer NG, Hany TF, Taverna C, et al. Non-Hodgkin's Lymphoma and Hodgkin's disease: co-registered FDG PET and CT at staging and restaging–do we need contrast-enhanced CT? Radiology 2004;232:823-9.
6. Antoch G, Freudenberg LS, Beyer T, Bockisch A, Debatin JF. To enhance or not to enhance? 18F-FDG and CT contrast agents in dual-modality 18F-FDG PET/CT. J Nucl Med 2004;45 Suppl 1:56S-65S.
7. Antoch G, Freudenberg LS, Stattaus J, et al. Whole-body positron emission tomography-CT: optimized CT using oral and IV contrast materials. AJR Am J Roentgenol 2002;179: 1555-60.
8. Antoch G, Kuehl H, Kanja J, et al. Dual-modality PET/CT scanning with negative oral contrast agent to avoid artifacts: introduction and evaluation. Radiology 2004;230:879-85.
9. Nanni C, Rubello D, Castellucci P, et al. 18F-FDG PET/CT fusion imaging in paediatric solid extracranial tumours. Biomed Pharmacother 2006;60:593-606.
10. Hernandez-Pampaloni M, Takalkar A, Yu JQ, Zhuang H, Alavi A. F-18 FDG-PET imaging and correlation with CT in staging and follow-up of pediatric lymphomas. Pediatr Radiol 2006;36:524-31.
11. Miller E, Metser U, Avrahami G, et al. Role of 18F-FDG PET/CT in staging and follow-up of lymphoma in pediatric and young adult patients. J Comput Assist Tomogr 2006;30:689-94.
12. Furth C, Denecke T, Steffen I, et al. Correlative imaging strategies implementing CT, MRI, and PET for staging of childhood Hodgkin disease. J Pediatr Hematol Oncol 2006;28: 501-12.
13. Arush MW, Israel O, Postovsky S, et al. Positron emission tomography/computed tomography with (18)fluoro-deoxyglucose in the detection of local recurrence and distant metastases of pediatric sarcoma. Pediatr Blood Cancer 2007;.
14. Ben Arush MW, Bar Shalom R, Postovsky S, et al. Assessing the use of FDG-PET in the detection of regional and metastatic nodes in alveolar rhabdomyosarcoma of extremities. J Pediatr Hematol Oncol 2006;28:440-5.
15. Kavanagh PV, Stevenson AW, Chen MY, Clark PB. Nonneoplastic diseases in the chest showing increased activity on FDG PET. AJR Am J Roentgenol 2004;183:1133-41.
16. Blodgett TM, Casagranda B, Townsend DW, Meltzer CC. Issues, controversies, and clinical utility of combined PET/CT imaging: what is the interpreting physician facing? AJR Am J Roentgenol 2005;184:S138-45.
17. Schoder H, Gonen M. Screening for Cancer with PET and PET/CT: Potential and Limitations. J Nucl Med 2007;48 Suppl 1:4S-18S.
18. Daldrup-Link HE, Franzius C, Link TM, et al. Whole-body MR imaging for detection of bone metastases in children and young adults: comparison with skeletal scintigraphy and FDG PET. AJR Am J Roentgenol 2001;177:229-36.
19. Goo HW, Yang DH, Ra YS, et al. Whole-body MRI of Langerhans cell histiocytosis: comparison with radiography and bone scintigraphy. Pediatr Radiol 2006;36:1019-31.
20. Hoffer FA. Magnetic resonance imaging of abdominal masses in the pediatric patient. Semin Ultrasound CT MR 2005;26:212-23.
21. Kellenberger CJ, Miller SF, Khan M, Gilday DL, Weitzman S, Babyn PS. Initial experience with FSE STIR whole-body MR imaging for staging lymphoma in children. Eur Radiol 2004;14:1829-41.
22. Kellenberger CJ, Epelman M, Miller SF, Babyn PS. Fast STIR whole-body MR imaging in children. Radiographics 2004;24:1317-30.
23. Laffan EE, O'Connor R, Ryan SP, V D. Whole-body magnetic resonance imaging: a useful additional sequence in paediatric imaging. Pediatr Radiol 2004;34:472-80.
24. Mazumdar A, Siegel MJ, V N, Luchtman-Jones L. Whole-body fast inversion recovery MR imaging of small cell neoplasms in pediatric patients: a pilot study. AJR Am J Roentgenol 2002;179:1261-6.

25. Walker RE, Eustace SJ. Whole-body magnetic resonance imaging: techniques, clinical indications, and future applications. Semin Musculoskelet Radiol 2001;5:5-20.
26. Eustace SJ, Walker R, Blake M, Yucel EK. Whole-body MR imaging. Practical issues, clinical applications, and future directions. Magn Reson Imaging Clin N Am 1999;7:209-36.
27. Siegel MJ, Luker GG. Bone marrow imaging in children. Magn Reson Imaging Clin N Am 1996;4:771-96.
28. Mentzel HJ, Kentouche K, Sauner D, et al. Comparison of whole-body STIR-MRI and 99mTc-methylene-diphosphonate scintigraphy in children with suspected multifocal bone lesions. Eur Radiol 2004;14:2297-302.
29. Levine DS, Navarro OM, Chaudry G, Doyle JJ, Blaser SI. Imaging the complications of bone marrow transplantation in children. Radiographics 2007;27:307-24.
30. Brenner D, Elliston C, Hall E, Berdon W. Estimated risks of radiation-induced fatal cancer from pediatric CT. AJR Am J Roentgenol 2001;176:289-96.
31. Lowe LH, Isuani BH, Heller RM, et al. Pediatric renal masses: Wilms' tumor and beyond. Radiographics 2000;20:1585-603.
32. Panicek DM, Go SD, Healey JH, Leung DH, Brennan MF, Lewis JJ. Soft tissue sarcoma involving bone or neurovascular structures: MR imaging prognostic factors. Radiology 1997;205:871-5.
33. Riccabona M. (Paediatric) magnetic resonance urography: just fancy images or a new important diagnostic tool? Curr Opin Urol 2007;17:48-55.
34. Nolte-Ernsting CC, Staatz G, Tacke J, Gunther RW. MR urography today. Abdom Imaging 2003;28:191-209.
35. Dowling C, Bollen AW, Noworolski SM, et al. Preoperative proton MR spectroscopic imaging of brain tumors: correlation with histopathologic analysis of resection specimens. AJNR Am J Neuroradiol 2001;22:604-12.
36. Hunter JV, Wang ZJ. MR spectroscopy in pediatric neuroradiology. Magn Reson Imaging Clin N Am 2001;9:165,89, ix.
37. Lazareff JA, Gupta RK, Alger J. Variation of post-treatment H-MRSI choline intensity in pediatric gliomas. J Neurooncol 1999;41:291-8.
38. Tzika AA, Zurakowski D, Poussaint TY, et al. Proton magnetic spectroscopic imaging of the child's brain: the response of tumors to treatment. Neuroradiology 2001;43:169-77.
39. Cha S, Lu S, Johnson G, Knopp EA. Dynamic susceptibility contrast MR imaging: correlation of signal intensity changes with cerebral blood volume measurements. J Magn Reson Imaging 2000;11:114-9.
40. Roberts HC, Roberts TP, Brasch RC, Dillon WP. Quantitative measurement of microvascular permeability in human brain tumors achieved using dynamic contrast-enhanced MR imaging: correlation with histologic grade. AJNR Am J Neuroradiol 2000;21:891-9.
41. Cha S, Knopp EA, Johnson G, Wetzel SG, Litt AW, Zagzag D. Intracranial mass lesions: dynamic contrast-enhanced susceptibility-weighted echo-planar perfusion MR imaging. Radiology 2002;223:11-29.
42. Cha S, Knopp EA, Johnson G, et al. Dynamic contrast-enhanced T2-weighted MR imaging of recurrent malignant gliomas treated with thalidomide and carboplatin. AJNR Am J Neuroradiol 2000;21:881-90.
43. Siegal T, Rubinstein R, Tzuk-Shina T, Gomori JM. Utility of relative cerebral blood volume mapping derived from perfusion magnetic resonance imaging in the routine follow up of brain tumors. J Neurosurg 1997;86:22-7.
44. Olsen OE, Sebire NJ. Apparent diffusion coefficient maps of pediatric mass lesions with free-breathing diffusion-weighted magnetic resonance: feasibility study. Acta Radiol 2006;47:198-204.
45. Humphries PD, Wynne CS, Sebire NJ, Olsen OE. Atypical abdominal paediatric lymphangiomatosis: diagnosis aided by diffusion-weighted MRI. Pediatr Radiol 2006;36:857-9.
46. Murtz P, Flacke S, Traber F, van den Brink JS, Gieseke J, Schild HH. Abdomen: diffusion-weighted MR imaging with pulse-triggered single-shot sequences. Radiology 2002;224:258-64.

47. Schubauer-Berigan MK, Daniels RD, Fleming DA, et al. Risk of chronic myeloid and acute leukemia mortality after exposure to ionizing radiation among workers at four U.S. nuclear weapons facilities and a nuclear naval shipyard. Radiat Res 2007;167:222-32.
48. Shuryak I, Sachs RK, Hlatky L, Little MP, Hahnfeldt P, Brenner DJ. Radiation-induced leukemia at doses relevant to radiation therapy: modeling mechanisms and estimating risks. J Natl Cancer Inst 2006;98:1794-806.
49. Steliarova-Foucher E, Stiller C, Lacour B, Kaatsch P. International Classification of Childhood Cancer, third edition. Cancer 2005;103:1457-67.
50. Amthauer H, Furth C, Denecke T, et al. FDG-PET in 10 children with Non-Hodgkin's Lymphoma: initial experience in staging and follow-up. Klin Padiatr 2005;217:327-33.
51. Collins CD. PET in lymphoma. Cancer Imaging 2006;6:S63-70.
52. Elstrom R, Guan L, Baker G, et al. Utility of FDG-PET scanning in lymphoma by WHO classification. Blood 2003;101:3875-6.
53. Friedberg JW, Fischman A, Neuberg D, et al. FDG-PET is superior to gallium scintigraphy in staging and more sensitive in the follow-up of patients with de novo Hodgkin lymphoma: a blinded comparison. Leuk Lymphoma 2004;45:85-92.
54. Guermazi A, Juweid ME. Commentary: PET poised to alter the current paradigm for response assessment of non-Hodgkin's lymphoma. Br J Radiol 2006;79:365-7.
55. Hermann S, Wormanns D, Pixberg M, et al. Staging in childhood lymphoma: differences between FDG-PET and CT. Nuklearmedizin 2005;44:1-7.
56. Montravers F, McNamara D, Landman-Parker J, et al. (18) FDG in childhood lymphoma: clinical utility and impact on management. Eur J Nucl Med Mol Imaging 2002;29:1155-65.
57. Rini JN, Nunez R, Nichols K, et al. Coincidence-detection FDG-PET versus gallium in children and young adults with newly diagnosed Hodgkin's disease. Pediatr Radiol 2005;35:169-78.
58. Willkomm P, Palmedo H, Grunwald F, Ruhlmann J, Biersack HJ. Functional imaging of Hodgkin's disease with FDG-PET and gallium-67. Nuklearmedizin 1998;37:251-3.
59. Juweid ME. Utility of Positron Emission Tomography (PET) Scanning in Managing Patients with Hodgkin's Lymphoma. Hematology Am Soc Hematol Educ Program 2006;:259-65.
60. Jhanwar YS, Straus DJ. The role of PET in lymphoma. J Nucl Med 2006;47:1326-34.
61. Kellenberger CJ, Epelman M, Miller SF, Babyn PS. Fast STIR whole-body MR imaging in children. Radiographics 2004;24:1317-30.
62. Frush DP, Donnelly LF, Rosen NS. Computed tomography and radiation risks: what pediatric health care providers should know. Pediatrics 2003;112:951-7.
63. Hsu SC, Metzger ML, Hudson MM, et al. Comparison of treatment outcomes of childhood Hodgkin's lymphoma in two US centers and a center in Recife, Brazil. Pediatr Blood Cancer 2006.
64. 2005-2006 Statistical Report: Primary Brain Tumors in the United States Statistical Report, 1998-2002 (Years Data Collected). Illinois, 2005 *(http://www.cbtrus.org/reports//2005-2006/2006report.pdf.)*.
65. Wang Z, Zimmerman RA, Sauter R. Proton MR spectroscopy of the brain: clinically useful information obtained in assessing CNS diseases in children. AJR Am J Roentgenol 1996;167:191-9.
66. Papaioannou G, McHugh K. Neuroblastoma in childhood: review and radiological findings. Cancer Imaging 2005;5:116-27.
67. Lonergan GJ, Schwab CM, Suarez ES, Carlson CL. Neuroblastoma, ganglioneuroblastoma, and ganglioneuroma: radiologic-pathologic correlation. Radiographics 2002;22:911-34.
68. Andrich MP, Shalaby-Rana E, Movassaghi N, Majd M. The role of 131 iodine-metaiodobenzylguanidine scanning in the correlative imaging of patients with neuroblastoma. Pediatrics 1996;97:246-50.
69. Gordon I, Peters AM, Gutman A, Morony S, Dicks-Mireaux C, Pritchard J. Skeletal assessment in neuroblastoma–the pitfalls of iodine-123-MIBG scans. J Nucl Med 1990;31:129-34.
70. Ritchey ML, Kelalis PP, Haase GM, Shochat SJ, Green DM, D'Angio G. Preoperative therapy for intracaval and atrial extension of Wilms tumor. Cancer 1993;71:4104-10.

71. Ritchey ML, Shamberger RC, Haase G, Horwitz J, Bergemann T, Breslow NE. Surgical complications after primary nephrectomy for Wilms' tumor: report from the National Wilms' Tumor Study Group. J Am Coll Surg 2001;192:63,8; quiz 146.
72. Grundy P, Perlman E, Rosen NS, et al. Current issues in Wilms tumor management. Curr Probl Cancer 2005;29:221-60.
73. Wilimas JA, Kaste SC, Kauffman WM, et al. Use of chest computed tomography in the staging of pediatric Wilms' tumor: interobserver variability and prognostic significance. J Clin Oncol 1997;15:2631-5.
74. Owens CM, Veys PA, Pritchard J, Levitt G, Imeson J, Dicks-Mireaux C. Role of chest computed tomography at diagnosis in the management of Wilms' tumor: a study by the United Kingdom Children's Cancer Study Group. J Clin Oncol 2002;20:2768-73.
75. Rohrschneider WK, Weirich A, Rieden K, Darge K, Troger J, Graf N. US, CT and MR imaging characteristics of nephroblastomatosis. Pediatr Radiol 1998;28:435-43.
76. Gylys-Morin V, Hoffer FA, Kozakewich H, Shamberger RC. Wilms tumor and nephroblastomatosis: imaging characteristics at gadolinium-enhanced MR imaging. Radiology 1993;188:517-21.
77. Breitfeld PP, Meyer WH. Rhabdomyosarcoma: new windows of opportunity. Oncologist 2005;10:518-27.
78. Bernstein M, Kovar H, Paulussen M, et al. Ewing's sarcoma family of tumors: current management. Oncologist 2006;11:503-19.
79. Daldrup-Link HE, Franzius C, Link TM, et al. Whole-body MR imaging for detection of bone metastases in children and young adults: comparison with skeletal scintigraphy and FDG PET. AJR Am J Roentgenol 2001;177:229-36.